THE ANOMALOUS MAGNETIC MOMENT OF THE MUON AND SHORT-DISTANCE BEHAVIOUR OF QUANTUM ELECTRODYNAMICS

B. LAUTRUP* and E. de RAFAEL+
Institut des Hautes Etudes Scientifiques, 91 Bures-sur-Yvette

Received 27 September 1973 (Revised 13 November 1973)

Abstract: The leading contributions to the anomalous magnetic moment of the muon due to electron vacuum polarization corrections are governed by the short-distance behaviour of the photon propagator. It is found that the formulation of this relationship in terms of a Callan-Symanzik equation for the muon anomaly is extremely useful for an actual evaluation of the leading mass dependent terms (i.e., terms proportional to powers of $\log m_{\mu}/m_e$). This enables us to predict all the mass dependent terms from a large class of eighth-order Feynman diagrams, in addition to verifying previously calculated lower order contributions, without much calculational effort. We emphasize that "light-by-light" type contributions are not included in this calculation. We have also been able to evaluate the mass independent terms contributing to the muon anomaly from a more restricted class of Feynman diagrams,

1. Introduction

It has already been known for some time that there is an intimate relationship between the renormalization group [1-2] and some of the mass dependent terms (i.e., terms proportional to powers of $\log m_{\mu}/m_{\rm e}$ in the muon anomalous magnetic moment. The first systematic investigation of this relationship was done by Kinoshita [3] in connection with the calculation of part of the sixth-order contribution to the muon anomaly. Because of the renormalization group structure the calculation was reduced to simple algebra.

One source of mass dependent terms in the muon anomaly are muon vertex graphs with electron loop insertions in the photon propagators. Various examples are shown in fig. 1. Because of the large mass ratio, $m_{\mu}/m_{\rm e} \approx 200$, one expects that the asymptotic part of the electron loops will play a dominant role. In other

^{*} On leave of absence from the Niels Bohr-Institute, Copenhagen.

⁺ Permanent address from Dec. 1973, Centre de Physique Theorique, CNRS, 31 Chemin J. Aiguier, 13274-Marseille, Cedex 02, France.

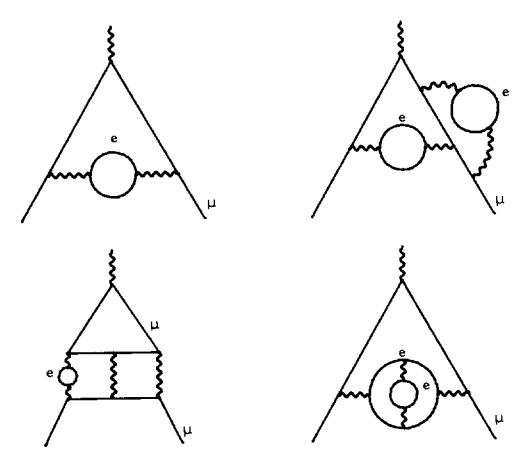


Fig. 1. Examples of graphs which give mass dependent terms to the muon anomaly.

words, one expects that the leading contributions to the muon anomaly from electron vacuum polarization corrections are governed by the short-distance behaviour of the photon propagator.

Recent years have seen great progress in the understanding of short-distance behaviour in field theory. It has been shown independently by Callan [4] and Symanzik [5] that the Green functions of any renormalizable field theory satisfy certain partial differential equations with respect to the masses and coupling constants. These so-called Callan-Symanzik equations are the local form of the global transformation laws taking the theory from one subtraction point to another. It is then perhaps not surprising, as will be shown below, that the part of the muon anomaly which is due to electron vacuum polarization corrections only, by itself, satisfies a Callan-Symanzik type equation, and that this equation, in the asymptotic regime where $m_{\rm e}/m_{\rm u} \rightarrow 0$, embodies all the renormalization group relations.

The last few years have also seen great progress in the calculations of the electron and muon anomalies, up to sixth-order *. This development has been motivated by a parallel improvement in the accuracy of the experiments **.

In the electron's case, the anomaly can be used to obtain an almost competitive value in accuracy for the fine structure constant. The forthcoming muon g-2 experiment at CERN will not only test our knowledge of quantum electrodynamics but also of numerous other effects, in particular the hadronic corrections ***. It

^{*} For a review of the situation (by the end of 1971) see ref. [6].

^{**} For a review of the experimental situation (by the beginning of 1972) see ref. [7].

^{***} For the most recent estimate of the hadronic corrections to $g_{\mu}-2$, where earlier references can be found, see ref. [8].

has been estimated [9] that the eighth-order contribution to the muon anomaly from mass dependent terms may be larger than the contribution due to weak interactions[†] and comparable to the future experimental precision. It would be nice, therefore, to have an exact calculation of these eighth-order mass dependent terms.

This paper is primarily devoted to a study of the short-distance behaviour of the photon propagator, in connection with the determination of the radiative corrections to a static quantity like the muon g-factor. We shall then use the powerful techniques of Callan-Symanzik equations for an explicit calculation of a large class of diagrams contributing to the muon anomaly in eighth-order. In contrast to the conventional renormalization group method [3], which treats classes of diagrams separately, the Callan-Symanzik formulation allows for a global calculation of mass dependent terms at a given order without having to consider the contributions from individual diagrams separately. We emphasize, however, that an important class of diagrams, i.e. those with light-by-light scattering insertions, cannot be estimated using this technique.

The paper is organized in the following way. In sect. 2 we present a short review of the theoretical and experimental situation concerning the anomalies, in order to spare the reader the trouble of searching the literature. In sect. 3 we derive the Callan-Symanzik equation for the muon anomaly and use it to calculate the mass dependent terms in eighth-order. For a more restricted class of diagrams we are even able to calculate the corresponding mass independent terms. This is done in sect. 4 for the electron vacuum polarization insertions into the lowest order muon vertex, and in sect. 5 for insertions into arbitrary muon vertices. In sect. 6 we summarize the results and present the conclusions. We have relegated to appendix A the more technical discussion of the correction terms to the asymptotic formulae used in the text. In appendix B we carry out explicitly the evaluation of the first three leading powers of $\log m_u/m_e$ to all orders of perturbation theory.

2. The lepton anomalies

The latest result in the long series of measurements of the electron g-2 is the one by Wesley and Rich [12], with the value *

$$a_e^{\text{exp}} = 0.0011596567(35).$$
 (2.1)

For the muon anomaly the latest experimental value obtained by the CERN group [14] is

$$a_{\mu}^{\text{exp}} = 0.00116616(31).$$
 (2.2)

[†] Our understanding of the weak contributions to $g_{\mu}-2$ has evolved considerably with the advent of the unified gauge theories of weak and electromagnetic interactions. For a review of the relevant calculations see refs. [10, 11].

^{*} This is the number given by Granger and Ford ref. [13] which corrects the previous value of Wesley and Rich ref. [12].

The next CERN experiment is expected to improve this number by a factor of 20 in the uncertainty.

The theoretical value for the electron anomaly is of the form

$$a_{\rm e}^{\rm QED} = A_1^{\rm e} \frac{\alpha}{\pi} + A_2^{\rm e} \left(\frac{\alpha}{\pi}\right)^2 + A_3^{\rm e} \left(\frac{\alpha}{\pi}\right)^3 + A_4^{\rm e} \left(\frac{\alpha}{\pi}\right)^4 + \dots, \tag{2.3}$$

where the coefficients are *

$$A_1^e = \frac{1}{2},$$
 (2.4)

$$A_2^e = \frac{197}{144} + \frac{\pi^2}{12} - \frac{1}{2} \pi^2 \log 2 + \frac{3}{4} \zeta(3) = -0.32848 \dots$$
 (2.5)

$$A_3^e = 1.29(6).$$
 (2.6)

The eighth-order coefficient A_4^e is totally unknown. It has contributions from 891 diagrams... The leading mass dependent term has been shown [16] to give a correction to the A_2^e coefficient which is

$$A_2^e \to A_2^e + \frac{1}{45} \left(\frac{m_e}{m_\mu}\right)^2 + O\left[\left(\frac{m_e}{m_\mu}\right)^4\right],$$
 (2.7)

and can therefore be disregarded at the present level of needed accuracy. From the first three powers of α/π in (2.3); and inserting the value [17]

$$\alpha^{-1} = 137.03608 (26),$$
 (2.8)

we find the theoretical prediction

$$a_e^{\text{th}} = 0.0011596529 (24)$$
 (2.9)

in reasonable agreement with the experimental value (2.1).

For the muon, the situation is as follows. The purely quantum electrodynamics effect is of the form

$$a_{\mu}^{\text{QED}} = A_{1}^{\mu} \left(\frac{\alpha}{\pi}\right) + A_{2}^{\mu} \left(\frac{\alpha}{\pi}\right)^{2} + A_{3}^{\mu} \left(\frac{\alpha}{\pi}\right)^{3} + A_{4}^{\mu} \left(\frac{\alpha}{\pi}\right)^{4} + \dots,$$
 (2.10)

^{*} For fourth order see ref. [29]. There are many contributors to sixth order; in particular there are three different evaluations of the bulk of the diagrams [15]. As we are not concerned with evaluating a current "best value" we have arbitrarily chosen the number quoted in ref. [15a], and warn the reader against misquotation of it. (See ref. [15] (or [6]) for the early history).

where the coefficients A_i^{μ} , $i = 2, 3, 4, \ldots$ depend now in a crucial way on the m_e/m_{μ} mass ratio. The corresponding numerical values are *:

$$A_1^{\mu} = \frac{1}{2},\tag{2.11}$$

$$A_2^{\mu} = 0.76578,\tag{2.12}$$

$$A_3^{\mu} = 23.0 \,(2).$$
 (2.13)

The large value of A_3^{μ} is essentially due to a new source of mass dependent terms, the light by light scattering contribution [18] shown in fig. 2. An educated guess [9] of the contribution to the eighth-order coefficient A_4^{μ} from all possible sources of mass dependent terms (469 diagrams) predicts

$$A_{\Delta}^{\mu} \sim 150 - 200. \tag{2.14}$$

Evaluating eq. (2.10) and adding the strong interaction contribution [8]

$$a_{\mu}^{\text{strong}} = 68 (9) \times 10^{-9},$$
 (2.15)

we find the theoretical prediction

$$a_{\mu}^{\text{th}} = 0.001165897 (10).$$
 (2.16)

We have here left out the estimated eighth-order contribution ($\sim 5 \times 10^{-9}$) and the weak contribution ($\sim 2 \times 10^{-9}$)**. The theoretical and experimental values agree within one standard deviation.

The next CERN experiment is expected to yield a precision better than 15×10^{-9} , in which case it begins to be of interest to have a more precise evaluation of the

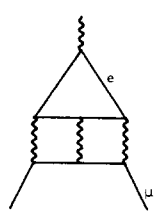


Fig. 2. Contribution to the muon anomaly from light by light scattering which gives the dominant contribution to the sixth-order coefficient $A\frac{M}{3}$.

^{*} For fourth order see ref. [26-28]. In sixth order a number of authors have been involved (see ref. [6] for the history and references). The number we quote is obtained from eq. (2.6) using the improved light-by-light value [19] and adding the result of ref. [15a] (see the previous footnote).

^{**} See footnote[†] page 3.

eighth-order contribution arising from the dominant mass dependent terms. The following sections are a step towards that goal.

3. The Callan-Symanzik equation for the muon anomaly

As mentioned in the introduction we shall limit ourselves to the type of Feynman diagrams shown in fig. 3, i.e. electron vacuum polarization insertions into a muon vertex. Specific examples are exhibited in fig. 1. These contributions are generated by replacing all internal photon lines in a renormalized muon vertex by dressed renormalized photon propagators of the form

$$-i\frac{g_{\mu\nu}}{q^2} \to -i\frac{g_{\mu\nu}}{q^2} d_{\rm R} (q^2/m_{\rm e}^2, \alpha) + q_{\mu}q_{\nu} \text{ terms.}$$
 (3.1)

The muon vertex may consist of a single graph, a subset of graphs or all graphs in a given order. It is understood however, that we are only considering sets of muon vertices that are gauge invariant under internal gauge transformations*. The function $d_{\rm R}(q^2/m_{\rm e}^2,\alpha)$ represents all electron loop corrections to the photon propagator. The muon vertex thus obtained, and hence the anomaly, a, becomes a functional of $d_{\rm R}$ of the form **

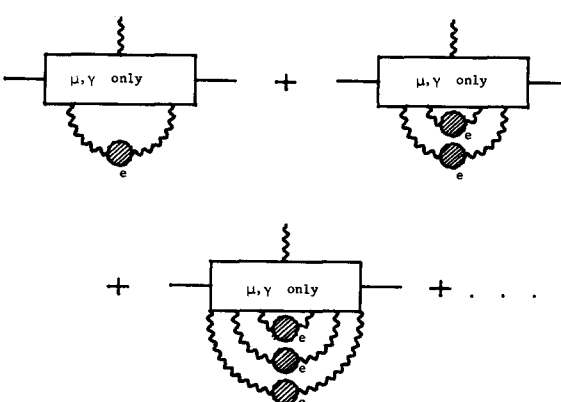


Fig. 3. Class of Feynman graphs contributing to the muon anomaly for which we shall write a Callan-Symanzik equation.

- * In this connection we would like to point out that it is commonly believed that such sets of muon vertices are also infrared convergent. The authors do not know, however, of a formal proof of this statement.
- ** Let us point out that the substitution (3.1) should also be carried out in the renormalization counterterms necessary to renormalize the original muon vertex. Thereby they become functionals of d_R as well as functions of a cut-off, Λ . When the (substituted) counterterms are added to the (substituted) unrenormalized contributions that also depend on Λ , the cut-off dependence must cancel and we arrive at the finite functional in eq. (3.2).

$$a = \phi(m_u^2, \{\alpha \, d_R(q^2/m_e^2, \alpha)\}_{q^2}), \tag{3.2}$$

where we have used curly brackets with a subscript q^2 to indicate that φ is a function of the whole expression within the brackets for all values of q^2 . We have also explicitly indicated the dependence on the muon mass, m_{μ} , the electron mass, $m_{\rm e}$, and the coupling constant, α . The functional φ does not itself have any dependence on α , because each propagator is associated with a factor e, at each end, which is taken care of by the factor α inside the brackets. If we put $d_{\rm R}=1$ in eq. (3.2) it reduces to the anomaly due to the original renormalized muon vertex. We are interested in the structural properties of this functional in the limit $m_{\rm e}/m_{\mu} \to 0$.

The photon propagator αd_R satisfies a Callan-Symanzik equation of the form [20]

$$\left[m_{\rm e} \frac{\partial}{\partial m_{\rm e}} + \beta(\alpha) \alpha \frac{\partial}{\partial \alpha} \right] \alpha d_{\rm R}(q^2/m_{\rm e}^2, \alpha) = \alpha \Delta(q^2/m_{\rm e}^2, \alpha), \tag{3.3}$$

where Δ is a function that vanishes for $q^2 \to -\infty$ or, equivalently, for $m_e \to 0$. This equation is obtained by studying the photon propagator's response to small variations in the physical (renormalized) mass, m, while keeping the unrenormalized coupling constant, α_0 , fixed [20]. Such a variation (the right hand side) may be expressed in terms of a variation of the physical mass, while keeping the physical coupling, α , fixed, plus the remaining variation of the physical coupling (the left hand side). On the other hand $\alpha d_R(q^2/m^2, \alpha)$ is the invariant charge which for fixed α_0 only depends on m via the unrenormalized mass m_0 . As m_0 only occurs in the denominator of the free electron propagator a variation must (by power counting) necessarily improve the asymptotic behaviour compared to the asymptotic behaviour of αd_R , which is logarithmic. Hence the right hand side must order by order vanish for $q^2 \to -\infty$. The function $\beta(\alpha)$ is finite in each order of perturbation theory and known explicitly up to sixth order [21],

$$\beta(\alpha) = \frac{2}{3} \frac{\alpha}{\pi} + \frac{1}{2} \left(\frac{\alpha}{\pi}\right)^2 - \frac{121}{144} \left(\frac{\alpha}{\pi}\right)^3 + \dots$$
 (3.4)

If we apply the operator $m_{\rm e} \, \partial/\partial m_{\rm e} + \beta\alpha\partial/\partial\alpha$ to the anomaly defined in eq. (3.2) it will only act at the $\, \alpha \, d_{\rm R} \,$ part and we find

$$\left(m_{\rm e} \frac{\partial}{\partial m_{\rm e}} + \beta(\alpha) \alpha \frac{\partial}{\partial \alpha}\right) a \left(\frac{m_{\mu}}{m_{\rm e}}, \alpha\right) = \Phi(m_{\mu}^2, \alpha d_{\rm R}, \alpha \Delta), \tag{3.5}$$

where Φ is a new functional, proportional to α Δ . (It is simply the integral over the functional derivative of φ with respect to α d_R , multiplied by $\alpha\Delta$.) Therefore the contribution to the muon anomaly from electron vacuum polarization insertions obeys a Callan-Symanzik type equation. The predictive power of eq. (3.5) rests on the fact that the ratio of the physical masses m_μ/m_e is large, and, therefore, to a good approximation, the study of this equation in the asymptotic regime $m_e/m_\mu \rightarrow 0$ will suffice for our purposes.

The crucial step towards simplicity is the fact that the vanishing of $\alpha\Delta$ in the limit $m_{\rm e} \to 0$ entails the vanishing of the right hand side of eq. (3.5). The proof of this, and in particular the estimate of how fast the r.h.s. vanishes, requires a rather technical analysis and we therefore relegate it to appendix A. Let us then consider eq. (3.5) in the asymptotic region $m_{\rm e}/m_{\mu} \to 0$. The asymptotic part of the anomaly, $a^{\infty}(m_{\mu}/m_{\rm e}, \alpha)$, is defined in the following way. In each order of perturbation theory we let $m_{\mu}/m_{\rm e} \to \infty$ and drop all terms that vanish in this limit. Divergent and constant terms are kept. As we shall see below the divergent terms are at most logarithmic so that we have

$$a^{\infty}\left(\frac{m_{\mu}}{m_{e}},\alpha\right) = B(\alpha) + C(\alpha)\log\frac{m_{\mu}}{m_{e}} + D(\alpha)\log^{2}\frac{m_{\mu}}{m_{e}} + E(\alpha)\log^{3}\frac{m_{\mu}}{m_{e}} + \dots,$$
(3.6)

where $B(\alpha)$, $C(\alpha)$, ... are power series in α . The asymptotic part of the anomaly obeys a homogeneous Callan-Symanzik equation

$$\left(m_e \frac{\partial}{\partial m_e} + \beta(\alpha) \alpha \frac{\partial}{\partial \alpha}\right) a^{\infty} \left(\frac{m_{\mu}}{m_e}, \alpha\right) = 0. \tag{3.7}$$

The solution to this equation is

$$a^{\infty}\left(\frac{m_{\mu}}{m_{e}},\alpha\right) = \left(\frac{m_{\mu}}{m_{e}}\right)^{\beta(\alpha)\alpha\partial/\partial\alpha}B(\alpha)$$

$$=\sum_{n=0}^{\infty} \log^{n} \frac{m_{\mu}}{m_{e}} \frac{1}{n!} \left(\beta(\alpha) \alpha \frac{\partial}{\partial \alpha} \right)^{n} B(\alpha), \tag{3.8}$$

where $B(\alpha)$ in principle is arbitrary, but by comparison with eq. (3.6) is seen to be simply the constant term in the asymptotic anomaly, i.e.,

$$B(\alpha) = a^{\infty} \left(\frac{m_{\mu}}{m_{\rm e}}, \alpha \right) \bigg|_{m_{\mu} = m_{\rm e}}$$
 (3.9)

From eq. (3.7) it is clear that only logarithms may occur in the asymptotic anomaly as demonstrated explicitly by eq. (3.8). It is also clear that the power of the logarithm is always smaller than that of α , because both β and B vanish for $\alpha = 0$. We can then write eq. (3.6) in a more explicit fashion

$$\alpha^{\infty} \left(\frac{m_{\mu}}{m_{e}}, \alpha \right) = \frac{\alpha}{\pi} \{B_{1}\}$$

$$+ \left(\frac{\alpha}{\pi} \right)^{2} \left\{ B_{2} + C_{2} \log \frac{m_{\mu}}{m_{e}} \right\}$$

$$+ \left(\frac{\alpha}{\pi}\right)^{3} \left\{B_{3} + C_{3} \log \frac{m_{\mu}}{m_{e}} + D_{3} \log^{2} \frac{m_{\mu}}{m_{e}}\right\}$$

$$+ \left(\frac{\alpha}{\pi}\right)^{4} \left\{B_{4} + C_{4} \log \frac{m_{\mu}}{m_{e}} + D_{4} \log^{2} \frac{m_{\mu}}{m_{e}} + E_{4} \log^{3} \frac{m_{\mu}}{m_{e}}\right\} + \dots, \quad (3.10)$$

where we have expanded the functions in powers of α/π . By comparison with eq. (2.10) we see that the expressions in the curly brackets are contributions to the coefficients A_n^{μ} . Our aim is to spell out the regularities among the coefficients B, C, D, E, \ldots and to show that they may be easily obtained from a knowledge of $\beta(\alpha)$ and $B(\alpha)$.

Once $B(\alpha)$ and $\beta(\alpha)$ are known, the complete asymptotic part of the anomaly is determined. In perturbation theory, knowledge of $B(\alpha)$ and $\beta(\alpha)$ up to a given order in α , say n, entails the knowledge of the coefficients of the n leading logarithms in any higher order. This is entirely similar to the renormalization group predictions in the case of asymptotic vacuum polarization. Comparing eqs. (3.6) and (3.8) we find

$$C(\alpha) = \beta(\alpha) \alpha \frac{\partial}{\partial \alpha} B(\alpha), \tag{3.11}$$

$$D(\alpha) = \frac{1}{2!} \left(\beta(\alpha) \alpha \frac{\partial}{\partial \alpha} \right)^2 B(\alpha) = \frac{1}{2} \beta(\alpha) \alpha \frac{\partial}{\partial \alpha} C(\alpha), \tag{3.12}$$

$$E(\alpha) = \frac{1}{3!} \left(\beta(\alpha) \alpha \frac{\partial}{\partial \alpha} \right)^3 B(\alpha) = \frac{1}{3} \beta(\alpha) \alpha \frac{\partial}{\partial \alpha} D(\alpha). \tag{3.13}$$

In perturbation theory we have explicitly (denothing the coefficients of α/π in $\beta(\alpha)$ (eq. (3.4)) by β_n) up to eigth-order

$$C_2 = \beta_1 B_1, \tag{3.14}$$

$$C_3 = \beta_2 B_1 + 2\beta_1 B_2, \tag{3.15}$$

$$C_{A} = \beta_{3}B_{1} + 2\beta_{2}B_{2} + 3\beta_{1}B_{3}, \tag{3.16}$$

$$D_3 = \beta_1 C_2, \tag{3.17}$$

$$D_4 = \beta_2 C_2 + \frac{3}{2} \beta_1 C_3, \tag{3.18}$$

$$E_4 = \beta_1 D_3. (3.19)$$

The β 's are all known analytically [21]. Of the B's, B_1 and B_2 are known analytically [27–29]:

$$B_1 = \frac{1}{2},\tag{3.20}$$

$$B_2 = A_2^{e} - \frac{25}{36}$$

$$= \frac{97}{144} + \frac{\pi^2}{12} - \frac{1}{2} \pi^2 \log 2 + \frac{3}{4} \zeta(3) = -1.0229 \dots, \tag{3.21}$$

while B_3 is known partly analytically partly numerically. Using the tables in ref. [6] we find the numerical result [3, 16, 30, 35].

$$B_3 = A_3^e + 1.94(2) = 3.23(6),$$
 (3.22)

where in the last line we have used eq. (2.6). All the coefficients except C_4 may now be evaluated analytically

$$C_2 = \frac{1}{3},\tag{3.23}$$

$$C_3 = \frac{31}{27} + \frac{\pi^2}{9} - \frac{2}{3} \pi^2 \log 2 + \xi(3) = -1.1139...,$$
 (3.24)

$$C_4 = 5.02(12),$$
 (3.25)

$$D_3 = \frac{2}{9} , (3.26)$$

$$D_4 = \frac{71}{54} + \frac{\pi^2}{9} - \frac{2}{3} \pi^2 \log 2 + \zeta(3) = -0.9472 \dots, \tag{3.27}$$

$$E_4 = \frac{4}{27}. (3.28)$$

Inserting the values of the coefficients given above into (3.10) we finally find

$$a^{\infty} \left(\frac{m_{\mu}}{m_{\rm e}}, \alpha \right) = 0.5 \frac{\alpha}{\pi} + 0.7658 \left(\frac{\alpha}{\pi} \right)^2$$

+ 3.61 (6)
$$\left(\frac{\alpha}{\pi}\right)^3$$
 + $(B_4 + 22.3(6)) \left(\frac{\alpha}{\pi}\right)^4$ + ... (3.29)

As expected, we see that the eighth-order mass dependent terms from the class of Feynman graphs shown in fig. 3 are completely determined,

$$C_4 \log \frac{m_{\mu}}{m_e} + D_4 \log^2 \frac{m_{\mu}}{m_e} + E_4 \log^3 \frac{m_{\mu}}{m_e} = 22.3 (6).$$
 (3.30)

An amusing numerological feature of this calculation is the strong cancellation among the two leading logarithms

$$D_4 \log^2 \frac{m_{\mu}}{m_e} + E_4 \log^3 \frac{m_{\mu}}{m_e} = -4.47. \tag{3.31}$$

This is somewhat reminiscent of a similar cancellation among the leading logarithms in sixth-order

$$C_3 \log \frac{m_\mu}{m_e} + D_3 \log^2 \frac{m_\mu}{m_e} = 0.378,$$
 (3.32)

which was first observed by Kinoshita [3]. We find these cancellations sufficiently intriguing to warrant a detailed analysis of leading powers of $\log m_{\mu}/m_{\rm e}$ in perturbation theory. This is the motivation for the appendix B, where the sum of the first three leading powers of $\log m_{\mu}/m_{\rm e}$ to all orders in perturbation theory is carried out.

The exact value of the constant B_4 remains unknown. It contributes to the eighth-order *mass independent* terms of the anomaly and, presumably, to the presently needed accuracy, it can be disregarded. As we shall see in the next section it is possible, however, from a detailed analysis of certain classes of Feynman graphs, to get their corresponding contribution to B_4 without much computational effort.

4. Electron vacuum polarization insertions into the lowest order muon vertex

The purpose of this and the next section is to extract the maximal information about the eighth-order muon anomaly obtainable from our knowledge of the asymptotic vacuum polarization and the lower order anomalies. The method we have used in the previous section is such that, because of the lumping together of all diagrams at a given order, one loses some information about individual diagrams. In this and the next section we want to recover the lost information, whenever possible. As we shall see, we shall be able to say more about certain types of diagrams, notably the electron vacuum polarization insertions into the lowest order muon vertex (see fig. 4) which are the subject of the present section.

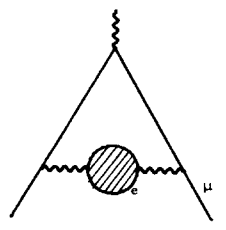


Fig. 4. Electron vacuum polarization insertion into the lowest muon vertex.

4.1. The asymptotic part of the photon propagator

The general expression for the renormalized photon propagator in quantum electrodynamics is

$$-iD_{\rm R}^{\mu\nu}(q) = -ig^{\mu\nu} \frac{d_{\rm R}(q^2/m_{\rm e}^2, \alpha)}{q^2} + q^{\mu}q^{\nu} \text{ terms.}$$
 (4.1)

As before, we shall disregard any contribution due to muon loops, and furthermore, we do not specify the precise nature of the longitudinal terms. Since the quantities we calculate are gauge invariant these terms will have no influence on the final result and we may consistently use only the $g_{\mu\nu}$ term in eq. (4.1).

It is convenient to express the function $d_{\mathbf{R}}$ in terms of the proper photon self-energy function $\pi_{\mathbf{R}}$,

$$d_{\rm R}(q^2/m_{\rm e}^2, \alpha) = \frac{1}{1 + \pi_{\rm R}(q^2/m_{\rm e}^2, \alpha)},\tag{4.2}$$

where

$$i\pi_{\rm R}^{\mu\nu}(q) = -i(g^{\mu\nu}q^2 - q^{\mu}q^{\nu})\,\pi_{\rm R}(q^2)$$
 (4.3)

is the sum of all proper renormalized self-energy diagrams contributing to the photon propagator (see fig. 5).

The asymptotic part of the photon's self-energy, $d_{\rm R}^{\infty}(q^2/m_{\rm e}^2, \alpha)$, for large space-like momenta is defined in exactly the same manner as the asymptotic part of the muon anomaly in the previous section. In each order of perturbation theory one lets $-q^2/m_{\rm e}^2 \rightarrow \infty$ and drops all terms that vanish in this limit. Divergent and constant terms are kept. Since the right hand side of eq. (3.3) vanishes for $q^2 \rightarrow -\infty$ the asymptotic propagator satisfies the Callan-Symanzik equation [20]

$$i \pi_{R}^{\mu\nu}(q) = +$$

+ . .

Fig. 5. The renormalized proper self-energy tensor $i\pi_{\mathbf{R}}^{\mu\nu}\left(q\right)$.

$$\left[m_{\rm e} \frac{\partial}{\partial m_{\rm e}} + \beta(\alpha) \alpha \frac{\partial}{\partial \alpha}\right] \alpha d_{\rm R}^{\infty} (q^2/m_{\rm e}^2, \alpha) = 0, \tag{4.4}$$

which, in complete analogy with the discussion in the previous section, shows that*

$$d_{\mathbf{R}}^{\infty}(q^2/m_{\mathbf{e}}^2, \alpha) = 1 + q(\alpha) + p(\alpha)\log(-q^2/m_{\mathbf{e}}^2) + r(\alpha)\log^2(-q^2/m_{\mathbf{e}}^2) + s(\alpha)\log^3(-q^2/m_{\mathbf{e}}^2) + \dots ,$$
(4.5)

where $q(\alpha), p(\alpha), \ldots$ are power series in α , of the form

$$1 + q(\alpha) = 1 + q_1 \frac{\alpha}{\pi} + q_2 \left(\frac{\alpha}{\pi}\right)^2 + q_3 \left(\frac{\alpha}{\pi}\right)^3 + \dots ,$$
 (4.6)

$$p(\alpha) = p_1 \frac{\alpha}{\pi} + p_2 \left(\frac{\alpha}{\pi}\right)^2 + p_3 \left(\frac{\alpha}{\pi}\right)^3 + \dots , \qquad (4.7)$$

$$r(\alpha) = r_2 \left(\frac{\alpha}{\pi}\right)^2 + r_3 \left(\frac{\alpha}{\pi}\right)^3 + \dots , \qquad (4.8)$$

$$s(\alpha) = s_3 \left(\frac{\alpha}{\pi}\right)^3 + \dots$$
 (4.9)

They are related to each other via the same kind of expressions as (3.11) - (3.13). This is, however, not very convenient from the point of view of calculating individual contributions to the anomaly. It is better then to express q, p, \ldots in terms of the coefficients of π_R^{∞} defined by

$$\pi_{\rm R}^{\infty}(q^2/m_{\rm e}^2, \alpha) = \frac{\alpha}{\pi} \left\{ a_1 + b_1 \log(-q^2/m_{\rm e}^2) \right\} + \left(\frac{\alpha}{\pi}\right)^2 \left\{ a_2 + b_2 \log(-q^2/m_{\rm e}^2) \right\} + \left(\frac{\alpha}{\pi}\right)^3 \left\{ a_3 + b_3 \log(-q^2/m_{\rm e}^2) + c_3 \log^2(-q^2/m_{\rm e}^2) \right\} + \dots$$

$$(4.10)$$

The structure of this equation follows from the solution of the Callan-Symanzik equation for $1 + \pi_R^{\infty}$ which may easily be obtained from eq. (4.4), i.e.,

$$1 + \pi_{R}^{\infty} (q^{2}/m_{e}^{2}, \alpha) = (-q^{2}/m_{e}^{2})^{\frac{1}{2}\beta(\alpha)(\alpha\partial/\partial\alpha - 1)} (1 + a(\alpha)), \tag{4.11}$$

where $a(\alpha) = a_1 \alpha/\pi + a_2(\alpha/\pi)^2 + ...$ is the value of π_R^{∞} for $q^2 = -m_e^2$. Then we find

$$b(\alpha) = \frac{1}{2} \beta(\alpha) \left(\alpha \frac{\partial}{\partial \alpha} - 1\right) (1 + a(\alpha)), \tag{4.12}$$

$$c(\alpha) = \frac{1}{4} \beta(\alpha) \left(\alpha \frac{\partial}{\partial \alpha} - 1 \right) b(\alpha), \qquad \dots$$
 (4.13)

^{*} The reader should be warned that here we deviate from Adler's notation, ref. [20]. This is to simplify notation in later calculations.

These equations contain all the renormalization group contraints, *. In particular, it follows from them that there is no $\log^2(-q^2/m_e^2)$ term in fourth-order (and in general, no $\log^p(-q^2/m_e^2)$ term in order α^p).

The known values of the coefficients in eq. (4.10) up to sixth order are:

$$b_1 = -\frac{1}{3},\tag{4.14}$$

$$a_1 = \frac{5}{9},\tag{4.15}$$

$$b_2 = -\frac{1}{4}$$
, (Jost-Luttinger, ref. [23]), (4.16)

$$a_2 = \frac{5}{24} - \zeta(3)$$
, (Hagen-Samuel, ref. [24], Lautrup-de Rafael ref. [16]), (4.17)

$$c_3 = -\frac{1}{2}b_1b_2 = -\frac{1}{24},\tag{4.18}$$

$$b_3 = \frac{47}{96} - \frac{1}{3} \zeta(3)$$
, Rosner ref. [25], de Rafael-Rosner. ref. [21]). (4.19)

The coefficient a_3 remains unknown.

From eq. (4.2) we can easily obtain the relationship between the coefficients q, p, \ldots and the coefficients a, b, \ldots Up to sixth-order they are

$$q_1 = -a_1,$$
 (4.20)

$$q_2 = -a_2 + a_1^2, (4.21)$$

$$q_3 = -a_3 + 2a_1a_2 - a_1^3, (4.22)$$

$$p_1 = -b_1,$$
 (4.23)

$$P_2 = -b_2 + 2a_1b_1, (4.24)$$

$$p_3 = -b_3 + 2(a_1b_2 + a_2b_1) - 3a_1^2b_1,$$
 (4.25)

$$r_2 = b_1^2$$
 , (4.26)

$$r_3 = \frac{1}{2}b_1b_2 + 2b_1b_2 - 3a_1b_1^2,$$
 (4.27)

$$s_3 = -b_1^3.$$
 (4.28)

We have tabulated the relationship among coefficients in such a way that it is easy to read off which contributions come from the proper graphs; which from the improper graphs consisting of two proper parts; and which from the improper graphs consisting of three proper graphs. This is explicitly illustrated in fig. 6.

^{*} For a discussion of these constraints, in connection with the Callan-Symanzik equation see, ref. [21].

Fig. 6. Classes of Feynman diagrams which up to sixth order contribute to the asymptotic photon-propagator $d_{\rm R}^{\infty}$ $(q^2/m^2, \alpha)$. Their corresponding contribution in terms of coefficients a's, b's and $L \equiv \log{(-q^2/m_{\rm e}^2)}$ are depicted at the bottom of each class of diagrams. Dashes after a diagram indicate permutations of internal photon lines.

4.2. Vacuum polarization insertions into the lowest order vertex

We now turn to the diagrams depicted in fig. 4 and write a subtracted dispersion relation for the contribution to $d_{\rm R}(q^2/m_{\rm e}^2)$ in the form

$$\frac{d_{\rm R}(q^2/m_{\rm e}^2) - 1}{q^2} = \int_{4m_{\rm e}^2}^{\infty} \frac{\mathrm{d}t}{t} \frac{\frac{1}{\pi} \, \mathrm{Im} \, [\mathrm{d}_{\rm R}(t/m_{\rm e}^2) - 1]}{t - q^2} \,. \tag{4.29}$$

It is therefore clear that the contribution to the muon anomaly from such diagrams, which we shall call $a_{(2)}$, is of the form

$$a_{(2)} = \int_{4m_e^2}^{\infty} \frac{dt}{t} K(t/m_\mu^2) \frac{1}{\pi} \operatorname{Im} (1 - d_R(t/m_e^2)), \tag{4.30}$$

where $K(t/m_{\mu}^2)$ is the muon anomaly due to exchange of a heavy photon with mass squared t in the lowest order diagram*. A convenient parametric form of this function is,

$$K(t/m_{\mu}^{2}) = \frac{\alpha}{\pi} \int_{0}^{1} dx \frac{x^{2}(1-x)}{x^{2} + (1-x)t/m_{\mu}^{2}}.$$
 (4.31)

Introducing this expression in eq. (4.30) we find using the dispersion relation (4.29),

$$a_{(2)} = \frac{\alpha}{\pi} \int_{0}^{1} dx (1-x) \left[d_{R} \left(\frac{-x^{2}}{1-x} - \frac{m_{\mu}^{2}}{m_{e}^{2}} \right) - 1 \right].$$
 (4.32)

This is an exact expression which in principle can be used to calculate the exact mass dependence of the contributions to the muon anomaly from the diagrams under consideration**. Here, we are interested in the asymptotic contribution to the anomaly, for which we simply have

$$a_{(2)}^{\infty} \left(\frac{m_{\mu}}{m_{\rm e}}, \alpha\right) = \frac{\alpha}{\pi} \int_{0}^{1} dx (1-x) \left[d_{\rm R}^{\infty} \left(\frac{-x^2}{1-x} \frac{m_{\mu}^2}{m_{\rm e}^2}, \alpha\right) - 1\right].$$
 (4.33)

As can be seen from eq. (4.32) non-asymptotic contributions from the photon propagator are only of importance in the interval $0 < x \le m_{\rm e}/m_{\mu}$ and therefore will be at most of order $O(m_{\rm e}/m_{\mu})$. (This point is discussed more fully in appendix A.) We are now in the position to calculate $a_{(2)}^{\infty}(m_{\mu}/m_{\rm e}, \alpha)$ explicitly. Inserting the

We are now in the position to calculate $a_{(2)}^{\infty}(m_{\mu}/m_{\rm e},\alpha)$ explicitly. Inserting the expression (4.5) for the asymptotic photon propagator in eq. (4.33); and defining the integrals

$$I_N = \int_0^1 dx (1-x) \log^N \frac{x^2}{1-x}, \qquad (4.34)$$

we find, up to eighth order,

$$a_{(2)}^{\infty} \left(\frac{m_{\mu}}{m_{e}}, \alpha\right) = \frac{\alpha}{\pi} 8 I_{0} s(\alpha) \log^{3} \frac{m_{\mu}}{m_{e}} + \frac{\alpha}{\pi} [12 I_{1} s(\alpha) + 4 I_{0} r(\alpha)] \log^{2} \frac{m_{\mu}}{m_{e}}$$

^{*} The reader interested in a more detailed account can consult e.g. ref. [16].

^{**} In fact, an exact calculation of the 4th-order diagram in fig. 7a has been done by Erikson and Liu, ref. [26].

$$+ \frac{\alpha}{\pi} \left[6 I_2 \, s(\alpha) + 4 I_1 \, r(\alpha) + 2 I_0 \, p(\alpha) \right] \, \log \, \frac{m_\mu}{m_e}$$

$$+ \frac{\alpha}{\pi} \left[I_3 \, s(\alpha) + I_2 \, r(\alpha) + I_1 \, p(\alpha) + I_0 \, q(\alpha) \right]. \tag{4.35}$$

From this result we can clearly read-off the corresponding contributions to the coefficients $B(\alpha)$, $C(\alpha)$, . . . defined in eq. (3.6). The interesting thing is that now we have explicit information about the mass-independent coefficient $B(\alpha)$! The integrals I_N are all calculable. We find for the first four values of N

$$I_0 = \frac{1}{2},\tag{4.36}$$

$$I_1 = -\frac{5}{4},\tag{4.37}$$

$$I_2 = \frac{13}{4} + \frac{1}{3} \pi^2 = 6.540...,$$
 (4.38)

$$I_3 = -\frac{87}{8} - \frac{5}{2} \pi^2 - 6 \zeta(3) = -42.76...$$
 (4.39)

In order to find the explicit contribution to $a_{(2)}^{\infty}$ $(m_{\mu}/m_{\rm e}, \alpha)$ from any of the groups of Feynman diagrams shown in fig. 7 we have only to insert the corresponding values for the coefficients $q(\alpha), p(\alpha), \ldots$ in eq. (4.35). These values can be read-off from the corresponding vacuum polarization diagrams in fig. 6. We then obtain the following results:

Fourth-order

There is only one mass dependent diagram at fourth-order (fig. 7a). We find

$$a_{(2a)} = \left(\frac{\alpha}{\pi}\right)^2 \left\{-a_1 I_0 - b_1 I_1 - 2b_1 I_0 \log \frac{m_\mu}{m_e}\right\} = \left(\frac{\alpha}{\pi}\right)^2 \left\{-\frac{25}{36} + \frac{1}{3} \log \frac{m_\mu}{m_e}\right\}$$

$$= 1.083 \left(\frac{\alpha}{\pi}\right)^{2}, \qquad (4.40)$$

which is the well known result first obtained by Suura and Wichmann [27] and Peterman [28]*.

Sixth-Order

There are two types of diagrams, figs. 7b, 7c which correspond respectively to the proper and improper fourth-order vacuum polarization insertions. For the proper type contribution we have

^{*} See also the previous footnote.

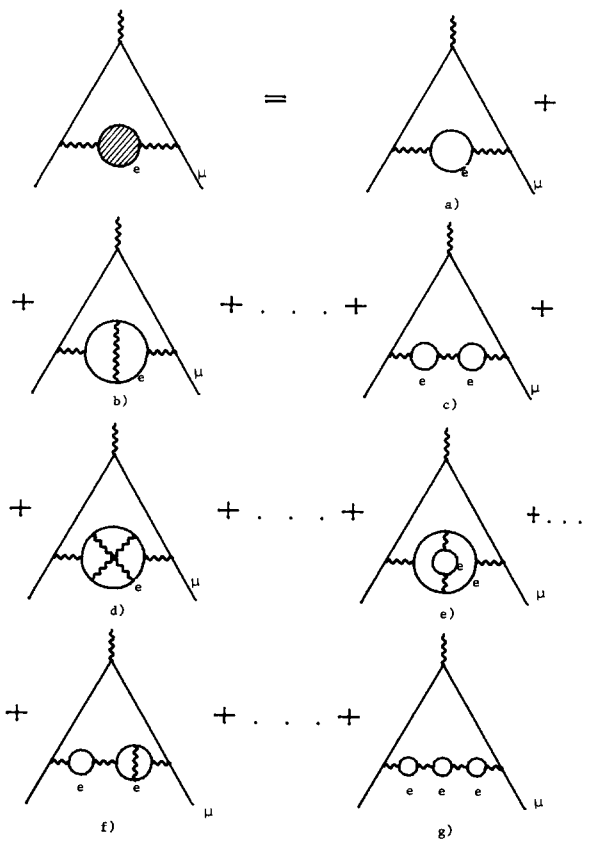


Fig. 7. Vacuum polarization insertions into the lowest order muon vertex: (a) fourth-order contribution; (b) and (c) sixth-order contribution; (d), (e), (f) and (g) eighth-order contribution.

$$a_{(2b)} = \left(\frac{\alpha}{\pi}\right)^{3} \left\{-a_{2}I_{0} - b_{2}I_{1} - 2b_{2}I_{0} \log \frac{m_{\mu}}{m_{e}}\right\}$$

$$= \left(\frac{\alpha}{\pi}\right)^{3} \left[-\frac{5}{12} + \frac{1}{2}\zeta(3) + \frac{1}{4} \log \frac{m_{\mu}}{m_{e}}\right] = 1.517 \left(\frac{\alpha}{\pi}\right)^{3}, \tag{4.41}$$

which is the result first obtained by Lautrup and de Rafael [16] using dispersion methods only.

For the improper type contribution we have

$$a_{(2a)} = \left(\frac{\alpha}{\pi}\right)^{3} \left\{a_{1}^{2} I_{0} + 2 a_{1} b_{1} + b_{1}^{2} I_{2} + (4a_{1} b_{1} I_{0} + 4b_{1}^{2} I_{1}) \log \frac{m_{\mu}}{m_{e}} + 4b_{1}^{2} I_{0} \log^{2} \frac{m_{\mu}}{m_{e}}\right\}$$

$$= \left(\frac{\alpha}{\pi}\right)^{3} \left\{\frac{317}{324} + \frac{\pi^{2}}{27} - \frac{25}{27} \log \frac{m_{\mu}}{m_{e}} + \frac{2}{9} \log^{2} \frac{m_{\mu}}{m_{e}}\right\}$$

$$= 2.724 \left(\frac{\alpha}{\pi}\right)^{3}, \tag{4.42}$$

which is the result first obtained by Kinoshita [3].

Eighth-order

In eighth-order there are two types of improper vacuum polarization insertions, which give contributions as indicated in figs. 7f and 7g, and two types of proper insertions: one-fermion loop type, which give contributions as shown in fig. 7d, and two-fermion loop type, which give contributions as shown in fig. 7e.

There are altogether 18 proper diagrams (15 of the one-loop type, fig. 7d; 3 of the two-loop type, fig. 7e). Their total contribution to the muon anomaly is

$$a_{(2d,e)} = \left(\frac{\alpha}{\pi}\right)^4 \left\{-a_3 I_0 - b_3 I_1 - c_3 I_2 - (2b_3 I_0 + 4c_3 I_1) \log \frac{m_\mu}{m_e} - 4c_3 I_0 \log^2 \frac{m_\mu}{m_e}\right\}. \tag{4.43}$$

Everything except a_3 is known here. Evaluating what we can, we get

$$a_{(2d,e)} = \left(\frac{\alpha}{\pi}\right)^4 \left\{-\frac{1}{2} a_3 + \frac{287}{384} + \frac{\pi^2}{72} - \frac{5}{12} \zeta(3) + \left(-\frac{67}{96} + \frac{1}{3} \zeta(3)\right) \log \frac{m_{\mu}}{m_{e}} + \frac{1}{12} \log^2 \frac{m_{\mu}}{m_{e}}\right\} = \left(\frac{\alpha}{\pi}\right)^4 \left\{-\frac{1}{2} a_3 + 1.168\right\}.$$

$$(4.44)$$

It would be interesting to know a_3 (see eq. (4.10)), which presumably contains higher transcendentals.

There are 6 diagrams of the improper class shown in fig. 7f. their total contribution to the muon anomaly is

$$a_{(2f)} = \left(\frac{\alpha}{\pi}\right)^{4} \left\{ 2a_{1} a_{2} I_{0} + 2(a_{1}b_{2} + b_{1}a_{2}) I_{1} + 2b_{1}b_{2}I_{2} + \left[4(a_{1}b_{2} + b_{1}a_{2}) I_{0} + 8b_{1}b_{2}I_{1}\right] \log \frac{m_{\mu}}{m_{e}} + 8b_{1}b_{2}I_{0} \log^{2} \frac{m_{\mu}}{m_{e}} \right\}$$

$$= \left(\frac{\alpha}{\pi}\right)^{4} \left\{ \frac{509}{432} + \frac{\pi^{2}}{18} - \frac{25}{18} \zeta(3) + \left[-\frac{5}{4} + \frac{2}{3} \zeta(3)\right] \log \frac{m_{\mu}}{m_{e}} + \frac{1}{3} \log^{2} \frac{m_{\mu}}{m_{e}} \right\}$$

$$= 7.140 \left(\frac{\alpha}{\pi}\right)^{4}. \tag{4.45}$$

We are left with the triple-bubble graph, fig. 7g, which is the only one contributing a $\log^3 m_\mu/m_e$ term to the anomaly, for which we find

$$a_{(2g)} = \left(\frac{\alpha}{\pi}\right)^{4} \left\{ -a_{1}^{3}I_{0} - 3a_{1}^{2}b_{1}I_{1} - 3a_{1}b_{1}^{2}I_{2} - b_{1}^{3}I_{3} + (-6a_{1}^{2}b_{1}I_{0} - 12a_{1}b_{1}^{2}I_{1} - 6b_{1}^{2}I_{2}) \log \frac{m_{\mu}}{m_{e}} + (-12a_{1}b_{1}^{2}I_{0} - 12b_{1}^{3}I_{1}) \log^{2} \frac{m_{\mu} - 8b_{1}^{3}I_{0}}{m_{e}} \log^{3} \frac{m_{\mu}}{m_{e}} \right\}$$

$$= \left(\frac{\alpha}{\pi}\right)^{4} \left\{ -\frac{8609}{5832} - \frac{25}{162}\pi^{2} - \frac{2}{9}\xi(3) + \left(\frac{317}{162} + \frac{2\pi^{2}}{27}\right) \log \frac{m_{\mu}}{m_{e}} - \frac{25}{27}\log^{2} \frac{m_{\mu} + \frac{4}{27}\log^{3} \frac{m_{\mu}}{m_{e}}}{m_{e}} \right\}$$

$$= 7.197 \left(\frac{\alpha}{\pi}\right)^{4}.$$

$$(4.46)$$

We see that we have been able to extract the full contribution to the asymptotic eighth-order muon anomaly from all the improper sixth-order electron vacuum polarization corrections to the second-order muon vertex.

5. Single electron vacuum polarization insertions into arbitrary muon-vertices

We now turn to the more general case of vacuum polarization insertions into a single photon line in an arbitrary muon vertex. This is illustrated in fig. 8a. By similar argument as above we obtain again eq. (4.30) where K(t) is the anomaly due to muon diagrams with one heavy photon of mass \sqrt{t} , (fig. 8b). From inspection of the diagrams one sees that K(t) is analytic in t everywhere except on the negative real axis where it must have a cut. Furthermore since $K(t) \to 0$ for $t \to \infty$, we may write an unsubtracted dispersion relation for it *,

$$K(t) = \int_{-\infty}^{0} dt' \frac{1}{t' - t} \frac{1}{\pi} \operatorname{Im} K(t').$$
 (5.1)

* Notice that for $t \ge 0$

$$K(t) = \lim_{q^2 \to -0} F_2(q^2, t);$$

and $F_2(q^2,t)$ in pure Q.E.D. is real for $q^2 \le 0$ because of the absence of anomalous thresholds. The fact that $K(t) \to 0$ for $t \to \infty$ is equivalent to the fact that the anomaly is independent of a photon propagator cut-off.

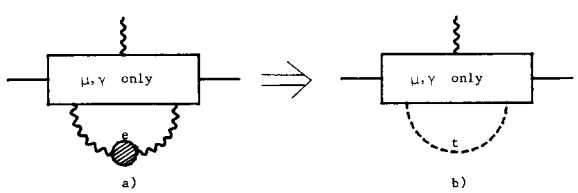


Fig. 8. (a) General structure of diagrams with electron vacuum polarization insertions in only one photon line; (b) the corresponding diagrams with a massive photon contributing to the function K(t).

It is useful to introduce the notation

$$\frac{1}{\pi} \operatorname{Im} K(t) = -k \left(-t/m_{\mu}^{2} \right) \left(\frac{\alpha}{\pi} \right)^{p}, \qquad (t < 0), \tag{5.2}$$

where we have factorized the quantity $(\alpha/\pi)^p$ which appears in $2p^{th}$ order. Then, the analogue of (4.33) is

$$a_{(2p)}^{\infty} \left(\frac{m_{\mu}}{m_{e}}, \alpha\right) = \left(\frac{\alpha}{\pi}\right)^{p} \int_{0}^{\infty} \frac{\mathrm{d}y}{y} k(y) \left[d_{R}^{\infty} \left(-y \frac{m_{\mu}^{2}}{m_{e}^{2}}\right) - 1\right]. \tag{5.3}$$

Terms neglected in using the asymptotic propagator arise from the region below and around $y = m_e^2/m_\mu^2$. From the fact that K(0) is finite we deduce that k(y) vanishes for $y \to 0$; and therefore the neglected terms vamish in the limit $m_e/m_\mu \to 0$ (see appendix A for more details.

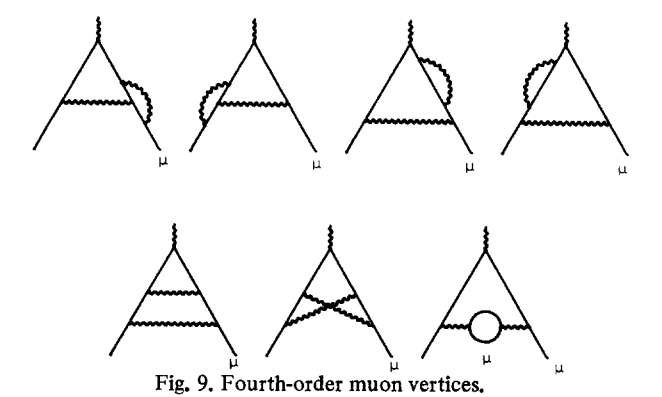
Introducing the explicit form of the asymptotic photon propagator into eq. (5.3) we obtain again an expression for the anomaly of the type written in eq. (4.35) except that now, the integrals I_N are

$$I_N = \int_0^\infty \frac{\mathrm{d}y}{y} \ k(y) \log^N y. \tag{5.4}$$

Except for N = 0 these integrals are not in general known analytically. For I_0 we have

$$\left(\frac{\alpha}{\pi}\right)^p I_0 = \left(\frac{\alpha}{\pi}\right)^p \int_0^\infty \frac{\mathrm{d}y}{y} k(y) = K(0), \tag{5.5}$$

which in $2p^{th}$ order is just p times the anomaly obtained from the corresponding diagrams without electron insertions. The reason for the factor p, is the p different photons into which we may insert the electron loops. We shall next discuss various applications of these formulas.



Draman County and an alasta and a state of the state of t

5.1. Proper fourth-order electron vacuum polarization insertions into the fourthorder muon vertices

There are altogether seven muon vertices in fourth-order (see fig. 9). Each muon vertex has two internal photon propagators i.e., two different ways to insert the three independent proper fourth-order electron vacuum polarization corrections. Altogether, this makes a total of 42 eighth-order Feynman diagrams (see fig. 10). For these diagrams we are able to extract the contribution to the asymptotic muon anomaly, mass independent terms included. Indeed, let us call $a_{(4,4)}^{\infty}(m_{\mu}/m_{e}, \alpha)$ their corresponding contribution. From eq. (5.3) we obtain

$$a_{(4,4)}^{\infty} \left(\frac{m_{\mu}}{m_{e}}, \alpha\right) = \left(\frac{\alpha}{\pi}\right)^{4} \left\{-a_{2}I_{0} - b_{2}I_{1} - 2b_{2}I_{0} \log \frac{m_{\mu}}{m_{e}}\right\}.$$
 (5.6)

The integral I_0 is known. It is twice the value of the fourth-order anomalous magnetic moment of the muon from the diagrams in fig. 9 i.e. *,

$$I_0 = 2 \left(\frac{197}{144} + \frac{\pi^2}{12} - \frac{1}{2} \pi^2 \log 2 + \frac{3}{4} \zeta(3) \right). \tag{5.7}$$

The integral I_1 is not known a priori. There is however one extra piece of information we have not used as yet, i.e., the contribution to the muon anomaly from second order electron vacuum polarization insertions into the fourth-order muon vertices. These sixth-order contributions are known **, partly analytically, partly numerically. If we call $a_{(4,2)}^{\infty}(m_{\mu}/m_{e},\alpha)$ their corresponding contribution to the anomaly, we have according to eq. (5.3),

$$a_{(4,2)}^{\infty} \left(\frac{m_{\mu}}{m_{e}}, \alpha \right) = \left(\frac{\alpha}{\pi} \right)^{3} \left\{ -a_{1} I_{0} - b_{1} I_{1} - 2b_{1} I_{0} \log \frac{m_{\mu}}{m_{e}} \right\},$$
 (5.8)

** For a detailed review of these calculations see ref. [6].

^{*} This is the famous analytic calcualtion of Peterman, ref. [28] and Sommerfield, ref. [29].

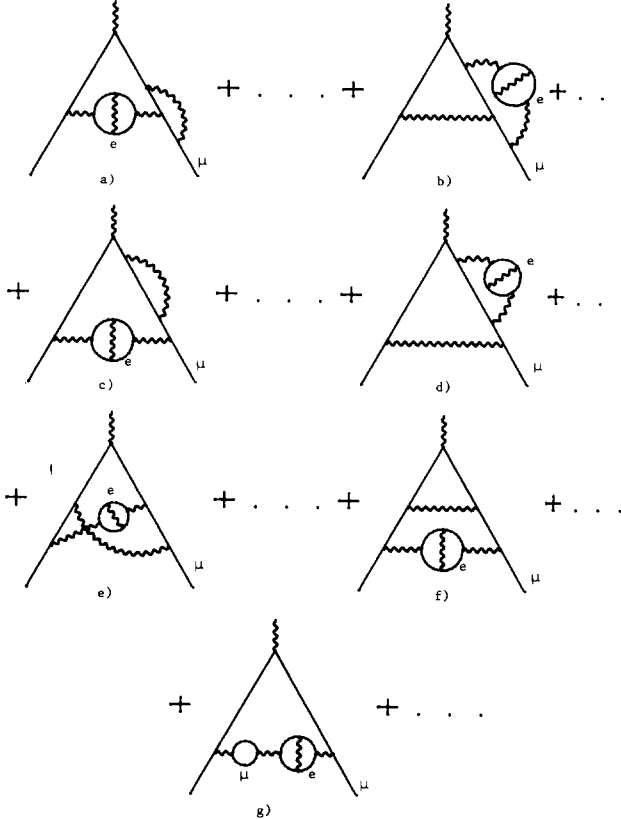


Fig. 10. Proper fourth-order electron vacuum polarization insertions into the fourth-order muon vertices.

where I_0 and I_1 are the same integrals as in eq. (5.6). The similar structure of eqs. (5.6) and (5.8) is due to the fact that second and fourth-order proper vacuum polarization insertions are both linear in $\log{(-q^2/m_e^2)}$ (see eq. (4.10)). The result of a direct calculation*, of $a_{(4,2)}^{\infty}(m_{\mu}/m_e, \alpha)$ is

$$a_{(4,2)}^{\infty} \left(\frac{m_{\mu}}{m_{e}}, \alpha\right) = \left(\frac{\alpha}{\pi}\right)^{3} \begin{cases} \frac{-61}{162} + \frac{\pi^{2}}{27} + \left(\frac{119}{27} - \frac{4}{9}\pi^{2}\right) \log \frac{m_{\mu}}{m_{e}} \\ + 0.04 \pm 0.05 + \left(-\frac{31}{12} + \frac{5}{9}\pi^{2} - \frac{2}{3}\pi^{2} \log 2 + \zeta(3)\right) \log \frac{m_{\mu}}{m_{e}} \end{cases}$$

$$(5.9)$$

The first line above corresponds to the contribution from the diagrams in fig. 11, which is known analytically [30], the second line to the other contributions** [35].

^{*} See footnote** of previous page.

^{**} There are other diagrams for which the constant terms have also been calculated analytically recently, see refs. [31, 32]. They do not however, constitute a gauge invariant subset.

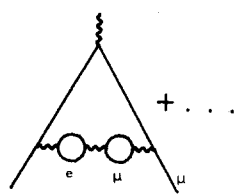


Fig. 11. The sixth-order diagrams for whicht he constant term in eq. (5.8) is known analytically. See ref. [30].

From the comparison between eqs. (5.8) and (5.9) we can get the values for the integrals I_0 and I_1 , corresponding to the analytically known part and the numerically known part separately. Upon substitution in eq. (5.6) we finally obtain

$$a_{(4,4)}^{\infty} \left(\frac{m_{\mu}}{m_{e}}, \alpha\right) = \left(\frac{\alpha}{\pi}\right)^{4} \begin{cases} \frac{473}{432} + \frac{119}{18} \zeta(3) - \frac{2}{3} \pi^{2} \zeta(3) + \left(\frac{119}{36} - \frac{1}{3} \pi^{2}\right) \log \frac{m_{\mu}}{m_{e}} \\ + 0.96(5) + \left(\frac{-31}{16} + \frac{5}{12} \pi^{2} \log^{2} + \frac{3}{4} \zeta(3)\right) \log \frac{m_{\mu}}{m_{e}} \end{cases}$$

$$(5.10)$$

where the first line corresponds to the contribution from the diagrams in fig. 10g and the second line to the total contribution from the other diagrams (figs. 10a-f). Numerically, we have

$$a_{(4,4)}^{\infty} \left(\frac{m_{\mu}}{m_{\alpha}}, \alpha \right) = \left(\frac{\alpha}{\pi} \right)^{4} \left\{ -7.554 + -0.87(5) \right\} = -8.43(5) \left(\frac{\alpha}{\pi} \right)^{4}.$$
 (5.11)

6. Summary of results and conclusions

We have shown that the electron vacuum polarization contributions to the muon anomaly satisfy a Callan-Symanzik equation, which allows us to predict the mass dependent terms from all such diagrams in eight-order as well as verifying lower order contributions. The mass independent terms could not be determined from the Callan-Symanzik equation alone. The input to the eighth-order calculation was the mass independent terms in the muon anomaly (known up to sixth-order) together with the β -function occurring in the Callan-Symanzik equation for the photon propagator (also known up to sixth-order). The calculation itself was reduced to simple algebra.

Using a slightly more detailed analysis we were able to calculate analytically the mass independent terms from the improper sixth-order electron vacuum polarization insertions into the second order vertex (the 7 diagrams in fig. 7f, g). We were also able to calculate the complete contribution from the proper sixth-order insertions (the 18 diagrams in fig. 7d, e) in terms of one unknown parameter, the constant term in the asymptotic vacuum polarization in sixth-order, Finally we were able to

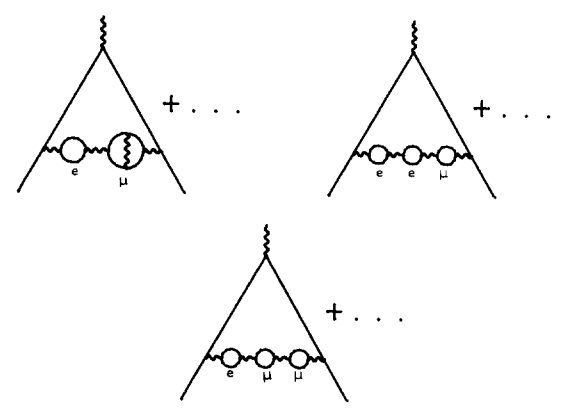


Fig. 12. Mixed double and triple bubble diagrams that may be evaluated at the expense of one (rather difficult) integral.

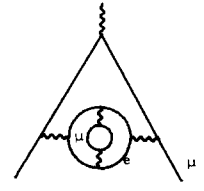
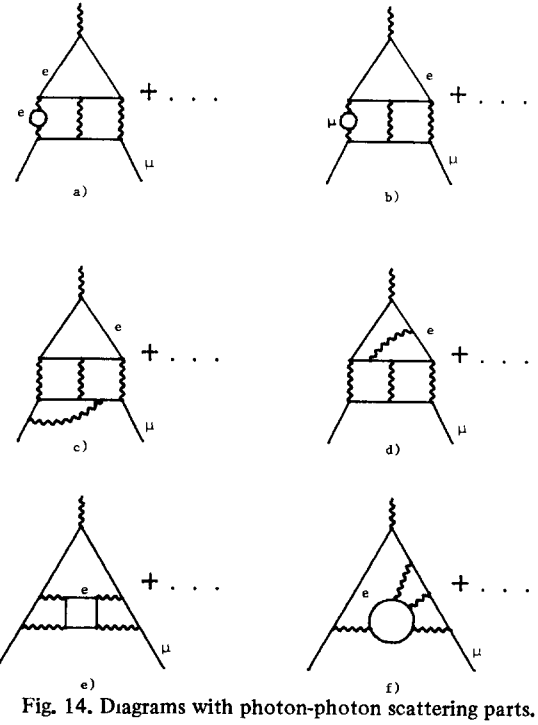


Fig. 13. A special kind of mixed vacuum polarization insertions.



determine numerically the constant term from the proper fourth-order electron vacuum polarization insertions into fourth-order vertices (the 42 diagrams in fig. 10). Thus, for 49 eighth-order diagrams the complete contribution is known. Only one diagram, the triple bubble in fig. 7g, required the evaluation of an unknown quantity, namely the integral in eq. (4.39). It is clear that at the expense of one integration (analytic or numeric) one may also use the techniques of sect. 5 to evaluate the mass independent terms from the 12 mixed double and triple bubble diagrams indicated in fig. 12.

There are altogether 1360 diagrams contributing to the eight-order muon anomaly. Of these, 891 only involve muons and are therefore identical to the corresponding electron contribution A_4^e about which nothing is known. Of the other 469 diagrams, we have calculated the mass dependent terms of all the electron vacuum polarization insertions (i.e., 304 diagrams)*. For 49 of these diagrams (the 7 diagrams in fig. 7f, g and the 42 diagrams in fig. 10) we have evaluated the constant terms as well. The remaining 165 diagrams are either a special kind of mixed vacuum polarization (fig. 13) or contain photon-photon scattering subgraphs (fig. 14) **. It is known [9] that the diagrams in fig. 14a could give a very large contribution, of the order of $180 (\alpha/\pi)^4$, ***. The diagrams in fig. 14b, c, d, are expected to be less important because they do not have a logarithm-generating electron vacuum polarization insertion. For the diagrams in fig. 14e, f, an application of Kinoshita's theorem on mass singularities [22, 33] indicates that they have no logarithmic dependence on the mass ratio. It is not clear whether the diagrams in fig. 13, have a logarithmic contribution.

The result of the contribution to the muon anomaly from the mass dependent terms of all the eighth-order diagrams that are electron vacuum polarization corrections, is

* This is the number of topologically distinct proper diagrams with non-zero contribution.

Writing

$$304 = 1 \times 72 \times 3 + (3 + 1) \times 7 \times 2 + (1 \times 1) \times 7 \times 1 + (18 + 6 + 1) \times 1 \times 1$$

we have first the contribution from a second order electron vacuum polarization insertions (1 diagram) into the sixth order muon vertex (72 diagrams). Each insertion can be done in 3 different ways. The next term is the contribution from fourth order (proper + improper) vacuum polarization in the fourth order vertex. Then follows the contribution from two second order insertions into two different lines of a fourth order vertex, and finally the sixth order insertion into the second order vertex.

** The number 165 is given by

$$165 = 3 + (3 + 3 + 8 + 10) \times 6 + 3 \times 6$$

corresponding to fig. 13 and figs. 14a-f respectively. Fig. 14a for instance is 3×6 because there are 3 ways of inserting the vacuum polarization blob into the 6 sixth order vertex diagrams with photon-photon scattering subgraphs. The diagrams in fig. 13 were not included in the discussion in ref. [9].

*** Barring for possible cancellations between leading logs of the type encountered in the electron vacuum polarization insertions.

$$\left(\frac{\alpha}{\pi}\right)^4 \left\{\frac{4}{27} \log^3 \frac{m_{\mu}}{m_{\rm e}} + \left[\frac{71}{54} + \frac{\pi^2}{9} - \frac{2}{3} \pi^2 \log 2 + \zeta(3)\right] \log^2 \frac{m_{\mu}}{m_{\rm e}} + 5.02(12) \log \frac{m_{\mu}}{m_{\rm e}}\right\} = 22.3 (6) \left(\frac{\alpha}{\pi}\right)^4.$$

Note added in proof

M. Samuel (Oklahoma State University preprint, November 1973) has recently independently reevaluated the 8th order anomaly using Kinoshita's method [3]. His results agree with ours where comparison is possible.

Appendix A. Proof of the Callan-Symanzik equation for the asymptotic anomaly

In this appendix we shall be concerned with the detailed derivation of the asymptotic Callan-Symanzik equation (3.7) from the non-asymptotic equation (3.5). From Weinberg's power counting theorem [34] it follows that for $q^2 \to -\infty$, the function $\Delta(q^2/m_e^2)$ vanishes as m_e^2/q^2 times possible powers of $\log q^2/m_e^2$. One would then naively expect that the r.h.s. of eq. (3.5) vanishes as m_e^2/m_μ^2 times powers of $\log m_\mu/m_e$ when $m_e \to 0$. That this is not the case is borne out by an explicit calculation of the fourth-order contribution to the muon anomaly from the Feynman diagram in fig. 7a. It is found [26] that

$$a_{(7a)} = \left(\frac{\alpha}{\pi}\right)^2 \left\{\frac{1}{3}\log\frac{m_{\mu}}{m_{e}} - \frac{25}{26} + \frac{\pi^2}{4}\frac{m_{e}}{m_{\mu}} + \ldots\right\},$$
 (A.1)

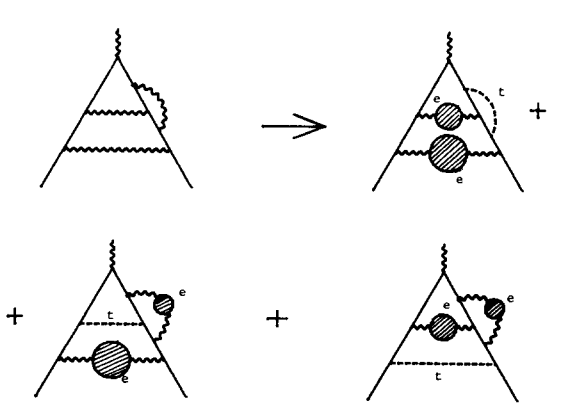


Fig. 15. Illustration of the type of diagrams that contribute to the evaluation of the right hand side of the Callan-Symanzik equation.

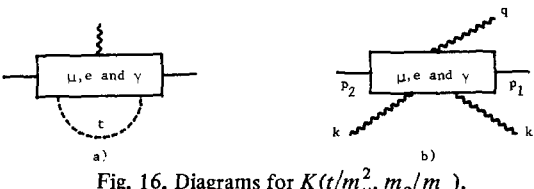


Fig. 16. Diagrams for $K(t/m_u^2, m_e/m_u)$.

i.e., the non-asymptotic terms are linear in the mass ratio and not quadratic. Hence, our naive expectations are wrong and a more careful analysis of the transition from eq. (3.5) to eq. (3.7) is required.

The right hand side $\Delta(q^2/m_e, \alpha)$ of the Callan-Symanzik equation for the photon propagator satisfies an unsubtracted dispersion relation in q^2

$$\Delta(q^2/m_{\rm e}^2) = \int_0^\infty \frac{{\rm d}t}{t - q^2} \frac{1}{\pi} \, {\rm Im} \, \Delta(t/m_{\rm e}^2). \tag{A.2}$$

This follows from eq. (4.29) by applying the Callan-Symanzik operator to both sides and using that for $q^2 \to -\infty$ we know that Δ vanishes. Let us denote the right hand side of eq. (3.5) by $R(m_e/m_u)$. Using the dispersion relation above for Δ we see that we may write

$$R\left(\frac{m_{\rm e}}{m_{\mu}}\right) = \int_{0}^{\infty} \frac{\mathrm{d}t}{t} \left[K\left(0, \frac{m_{\rm e}}{m_{\mu}}\right) - K\left(\frac{t}{m_{\mu}^{2}}, \frac{m_{\rm e}}{m_{\mu}}\right)\right] \times \frac{1}{\pi} \operatorname{Im} \Delta(t/m_{\rm e}^{2}), \tag{A.3}$$

where $K(t/m_{\mu}^2, m_{\rm e}/m_{\mu})$ is the anomalous magnetic moment from the diagrams where all photon propagators but one have been substituted according to (3.1) and the exceptional propagator has been given a photon mass \sqrt{t} . This is illustrated with an example in fig. 15. Scaling the t variable we may transfer all the dependence on $m_{\rm e}$ to the anomaly

$$R\left(\frac{m_{\rm e}}{m_{\rm \mu}}\right) = \int\limits_0^\infty \frac{\mathrm{d}x}{x} \frac{1}{\pi} \operatorname{Im} \Delta(x) \left\{ K\left(0, \frac{m_{\rm e}}{m_{\rm \mu}}\right) - K\left(x \frac{m_{\rm e}^2}{m_{\rm \mu}^2}, \frac{m_{\rm e}}{m_{\rm \mu}}\right) \right\}. \tag{A.4}$$

Since π^{-1} Im $\Delta(x)$ vanishes for $x \to \infty$ as 1/x (apart from logarithms) the integral is dominated by the small x behaviour of the integrand, i.e. by the way $K(t/m_u^2, m_e)$ m_{μ}) approaches $K(0, m_{\rm e}/m_{\mu})$ for $t \ll m_{\mu}^2$. The vertex function giving rise to $K(t/m_{\mu}^2, m_{\rm e}/m_{\mu})$ (fig. 16a) may be expressed

in terms of the double Compton amplitude $C_{\mu}(k, p_2, p_1)$ (fig. 16b)

$$V_{\mu}(p_2, p_1, t) = -i \int \frac{\mathrm{d}^4 k}{(2\pi)^4} \frac{C_{\mu}(k, p_2, p_1)}{k^2 - t} . \tag{A.5}$$

Then, the difference $K(0, m_e/m_\mu) - K(t/m_\mu^2, m_e/m_\mu)$ is given by

$$V_{\mu}(p_2, p_1, 0) - V_{\mu}(p_2, p_1, t) = ti \int \frac{\mathrm{d}^4 k}{(2\pi)^4} \frac{C_{\mu}(k, p_2, p_1)}{k^2 (k^2 - t)}. \tag{A.6}$$

The factor $t = x m_e^2/m_\mu^2$ in front of this integral reflects our naive expectation that R vanishes as m_e^2/m_μ^2 . This however can be masked by the possibility that the integral over k may diverge. Our aim is to estimate how badly it can diverge. The divergence is of the infrared type and we may use the usual power counting methods for estimating its strength. Thus, of the three types of diagrams shown in fig. 17 the one where the t-photon is attached to both the external legs, (c), is the most divergent; the one where only one end is attached to an external leg, (b), is less divergent while the one where the t-photon is attached to two internal vertices, (a), is the least divergent. Since the Fermion propagators $(p+k)^2 - m^2 = k^2 + 2n \cdot k$ are linear in k for $k \to 0$ we expect only type (c) to give a divergent contribution of the strength $d^4k/k^4 \sim \log t$ to the integral in eq. (A.5), while (a) and (b) are convergent. On the other hand we know that the anomalous magnetic moment extracted from eq. (A.5) by means of a suitable projection operator is convergent for t = 0, so the apparent logarithmic divergence of diagram (c) must somehow be cancelled in the anomaly. (We shall see in a moment that the terms responsible for this cancellation are the renormalization counterterms to the diagrams in fig. 17a). Turning now to the difference in eq. (A.6), we conclude that the leading divergence which is naively quadratic must also cancel here. Thus instead of behaving like $d^4k/k^6 \sim 1/t$ the divergent contribution to the anomaly of (A.6) from diagram (c) must behave like $d^4k/k^5 \sim 1/\sqrt{t}$ or better. Hence

$$K\left(0, \frac{m_{\rm e}}{m_{\rm u}}\right) - K\left(\frac{t}{m_{\rm u}}, \frac{m_{\rm e}}{m_{\rm u}}\right) \sim \frac{\sqrt{t}}{m_{\rm u}},$$
 (A.7)

apart from possible logarithmic factors. This implies via (A.4) that the leading behaviour of the r.h.s. in the Callan-Symanzik equation is of the form

$$R\left(\frac{m_{\rm e}}{m_{\mu}}\right) = \frac{m_{\rm e}}{m_{\mu}} F\left(\log \frac{m_{\mu}}{m_{\rm e}}\right). \tag{A.8}$$

The logarithms arise partly from the remaining vacuum polarization insertions and partly from possible logarithmic enhancements of the infrared behaviour of the blob insertions in fig. 17b and c.

Finally we shal show explicitly how the infrared divergence of the contribution to (A.5) from fig. 17c is cancelled by renormalisation subtractions. The corresponding vertex amplitude is

$$V_{\mu}^{(6)}(p_{2},p_{1}) = ie^{2} \int \frac{d^{4}k}{(2\pi)^{4}} \frac{\gamma_{\rho}(p_{2}+k+m_{\mu})W_{\mu}(p_{2}+k,p_{1}+k)(p_{1}+k+m_{\mu})\gamma^{\rho}}{(k^{2}+2p_{2}\cdot k)(k^{2}+2p_{1}\cdot k)(k^{2}-t)}, (A.9)$$

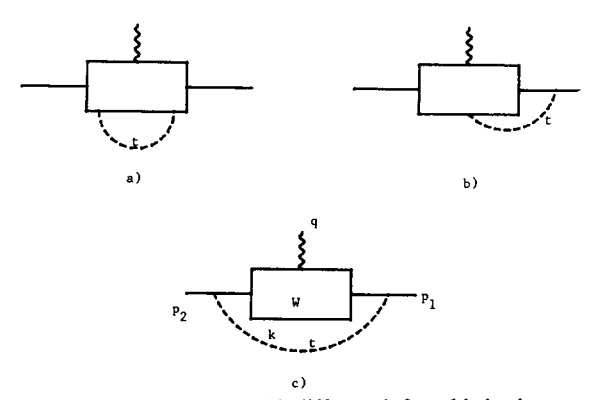


Fig. 17. Contributions with different infrared behaviours.

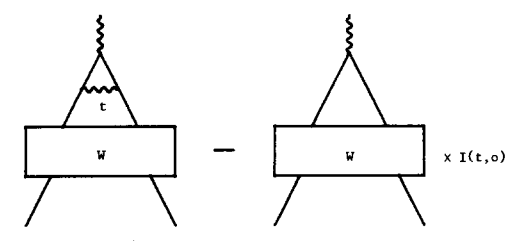


Fig. 18. Second order correction to the vertex where the external photon is attached, and its subtraction constant.

where W_{μ} is the vertex function of the blob in (fig. 17c). To isolate the infrared divergence we put k=0 in the numerator and use the Dirac equation to obtain

$$V_{\mu}^{(c)}(p_2, p_1) = W_{\mu}(p_2 p_1) I(t, q^2),$$
 (A.10)

where

$$I(t, q^{2}) = ie^{2} \int \frac{d^{4}k}{(2\pi)^{4}} \frac{4p_{1} \cdot p_{2}}{(k^{2} + 2p_{1} \cdot k)(k^{2} + 2p_{2} \cdot k)(k^{2} - t)}$$

$$= \frac{\alpha}{\pi} \int_{0}^{1} dx \int_{0}^{1} dy \frac{x(m_{\mu}^{2} - \frac{1}{2}q^{2})}{x^{2}(m_{\mu}^{2} - y(1 - y)q^{2}) + (1 - x)t}.$$
(A.11)

We clearly see the logarithmic divergence,

$$\int_{0}^{1} \frac{\mathrm{d}x}{x} \,, \text{ for } t = 0. \tag{A.12}$$

Because we work with a renormalized theory we must subtract the unrenormalized amplitudes. Although the unrenormalized diagrams of type (a) and (b) are infrared finite for $t \to 0$ this is not the case for the corresponding subtraction constants. In fig. 18 a diagram of this type is shown. The infrared part of the subtraction constant is just the integral in (A.11) at $q^2 = 0$, such that we have the complete infrared contribution to V_u

$$V_{\mu}(p_2, p_1) = W_{\mu}(p_2, p_1) (I(t, q^2) - I(t, 0)), \tag{A.13}$$

which vanishes in the static limit, $q^2 = 0$. We remark that the second order subtraction constants arising from other integral vertices are exactly cancelled by the electron propagator subtractions due to Ward's identity. Subtraction constants for higher than second order vertex corrections are not divergent for $t \to 0$ in the static limit.

Appendix B. Summation of leading logarithms

From the structure of the Callan-Symanzik equation it follows that if one knows β and B to p'th order in α/π then one can calculate the p leading logarithms in all orders. Writing

$$a^{\infty} \left(\frac{m_{\mu}}{m_{e}}, \alpha \right) = \sum_{p=1}^{\infty} \left(\frac{\alpha}{\pi} \right)^{p} \left\{ X_{p} \log^{p-1} \left(\frac{m_{\mu}}{m_{e}} \right) + Y_{p} \log^{p-2} \left(\frac{m_{\mu}}{m_{e}} \right) + Z_{p} \log^{p-3} \left(\frac{m_{\mu}}{m_{e}} \right) + \dots \right\}, \tag{B.1}$$

We find from the Callan-Symanzik equation (eq. (3.8)) the following recursion formulas for the coefficients X, Y and Z:

$$X_p = \beta_1 X_{p-1},$$
 (B.2)

$$Y_{p} = \beta_{1} \frac{p-1}{p-2} Y_{p-1} + \beta_{2} X_{p-2},$$
 (B.3)

$$Z_{p} = \beta_{1} \frac{p-1}{p-3} Z_{p-1} + \beta_{2} \frac{p-2}{p-3} Y_{p-2} + \beta_{3} X_{p-3},$$
 (B.4)

with the initial conditions

$$X_1 = B_1; \quad Y_2 = B_2; \qquad Z_3 = B_3.$$
 (B.5)

Solving eqs. (B.2) - (B.4) we find

$$X_p = \beta_1^{p-1} B_1, (B.6)$$

$$Y_p = (p-1)\beta_1^{p-2} B_2 + (p-1) \left(\sum_{k=2}^{p-1} \frac{1}{k}\right) \beta_2 \beta_1^{p-3} B_1,$$
 (B.7)

$$\begin{split} Z_p &= \frac{1}{2} (p-1)(p-2) \, \beta_1^{p-3} \, B_3 \\ &+ (p-1)(p-2) \, \binom{p - 1}{k = 3} \cdot \frac{1}{k} \beta_2 \beta_1^{p-4} \, B_2 \\ &+ \frac{1}{2} (p-2)(p-3) \, \beta_3 \beta_1^{p-4} \, B_1 \\ &+ (p-1) (p-2) \, \binom{p - 1}{k = 4} \, \binom{p - 2}{k = 2} \cdot \frac{1}{k \Omega} \beta_2^2 \, \beta_1^{p-5} \, B_1. \end{split} \tag{B.8}$$

We are now able to answer the question whether the two leading logarithms always tend to cancel each other. Let us define the ratio

$$R_{p} \equiv \frac{Y_{p}}{X_{p}} = (p-1)\frac{\beta_{2}}{\beta_{1}} \left(\sum_{k=2}^{p-1} \frac{1}{k} + \frac{\beta_{1}B_{2}}{\beta_{2}B_{1}} \right).$$
 (B.9)

The first numerical values are

$$R_2 = -3.07,$$
 (B.10)

$$R_3 = -5.01,$$
 (B.11)

$$R_4 = -6.39.$$
 (B.12)

Since $\log m_{\mu}/m_{\rm e} = 5.33$ this means that the two leading logarithms for small p tend to cancel. For $p \to \infty$ it is, however, evident that the ratio eventually will change sign and diverge as $+ p \log p$. The ratio reaches its minimum $R_{\rm min} = -9.10$ for p = -10 and becomes positive from p = 24 onwards.

The expressions for X, Y and Z look very summable. Instead of attempting a direct summation it is simpler to solve the Gell-Mann, Low equation for the effective fine structure constant $\overline{\alpha}(t)$,

$$\frac{\mathrm{d}\overline{\alpha}}{\mathrm{d}t} = \overline{\alpha} \ \beta(\overline{\alpha}),\tag{B.13}$$

with the boundary value $\overline{\alpha}$ $(t=0)=\alpha$. Then it is easily verified that the solution to the Callan-Symanzik equation (3.8) is

$$a^{\infty} \left(\frac{m_{\mu}}{m_{e}}, \alpha \right) = B(\overline{\alpha}(t))|_{t=\log m_{\mu}/m_{e}} = B_{1} \frac{\overline{\alpha}}{\pi} + B_{2} \left(\frac{\overline{\alpha}}{\pi} \right)^{2} + B_{3} \left(\frac{\overline{\alpha}}{\pi} \right)^{3} + \dots$$
 (B.14)

Eq. (B.13) may be solved for t

$$t = \int_{\alpha}^{\overline{\alpha}} \frac{\mathrm{d}x}{x\beta(x)},\tag{B.15}$$

which when expanded in leading powers of α and $\overline{\alpha}$ becomes

$$t = \frac{\pi}{\beta_1} \left(\frac{1}{\alpha} - \frac{1}{\overline{\alpha}} \right) - \frac{\beta_2}{\beta_1^2} \log \frac{\overline{\alpha}}{\alpha} + \left(\frac{\beta_2^2}{\beta_1^3} - \frac{\beta_3}{\beta_1^2} \right) \left(\frac{\overline{\alpha} - \alpha}{\pi} \right) + \dots$$
 (B.16)

This equation may be solved to higher and higher precision by a set of successive approximations. Keeping terms of order $\alpha^p t^p$, $\alpha^p t^{p-1}$ and $\alpha^p t^{p-2}$ we find with $z = (\alpha/\pi) \beta_1 t$

$$\frac{\overline{\alpha}}{\alpha} = \frac{1}{1-z} - \left(\frac{\alpha}{\pi}\right) \frac{\beta_2}{\beta_1} \frac{\log(1-z)}{(1-z)^2} + \left(\frac{\alpha}{\pi}\right)^2 \frac{\beta_2^2}{\beta_1^2} \frac{\log^2(1-z) - \log(1-z) - z}{(1-z)^3} + \left(\frac{\alpha}{\pi}\right)^2 \frac{\beta_3}{\beta_1} \frac{z}{(1-z)^3} + \dots$$
(B.17)

Inserting this into (B.14) we finally arrive at the summed up expression for the anomaly

$$a^{\infty} \left(\frac{m_{\mu}}{m_{e}}, \alpha\right) = \frac{\alpha}{\pi} \frac{B_{1}}{1-z} + \left(\frac{\alpha}{\pi}\right)^{2} \left(\frac{B_{2}}{(1-z)^{2}} - B_{1} \frac{\beta_{2}}{\beta_{1}} \frac{\log(1-z)}{(1-z)^{2}}\right) + \left(\frac{\alpha}{\pi}\right)^{3} \left(\frac{B_{3}}{(1-z)^{3}} - 2B_{2} \frac{\beta_{2}}{\beta_{1}} \frac{\log(1-z)}{(1-z)^{3}} + B_{1} \frac{\beta_{3}}{\beta_{1}} \frac{z}{(1-z)^{3}} + B_{1} \left(\frac{\beta_{2}}{\beta_{1}}\right)^{2} \frac{\log^{2}(1-z) - \log(1-z) - z}{(1-z)^{3}} + O\left(\left(\frac{\alpha}{\pi}\right)^{4} f(z)\right),$$
(B.18)

where $z = (\alpha/\pi) \beta_1 \log m_\mu/m_e$. This expression which is correct to three leading logarithms is of course equivalent to (B.6)—(B.8). The first term has previously been found by Terazawa [36].

References

- [1] E.C.G. Stueckelberg and A. Peterman, Helv. Phys. Acta 26 (1953) 499.
- [2] M. Gell-Mann and F.E. Low, Phys. Rev. 95 (1954) 1300.
- [3] T. Kinoshita, Nuovo Cimento 51B (1967) 140,
- [4] C. Callan, Jr., Phys. Rev. D2 (1970) 1541.
- [5] K. Symanzik, Comm. Math. Phys. 18 (1970) 227; 23 (1971) 49.
- [6] B. Lautrup, A. Peterman and E. de Rafael, Phys. Reports 3 (1972) 193.
- [7] A. Rich and J.C. Wesley, Revs. Mod. Phys. 44 (1972) 250.
- [8] A. Bramon, E. Etim and M. Greco, Phys. Letters 39B (1972) 514.
- [9] B. Lautrup, Phys. Letters 38B (1972) 408.
- [10a] J. Primack, Proceedings of the 16th Int. Conf. on high energy physics, NAL, 1972.
- [10b] J. Primack and H. Quinn, Phys. Rev. D6 (1972) 3171.
- [11] B. Lautrup, Proceedings of the Rencontre de Moriond, Meribel-lès -Allues, 1973.

- [12] J.C. Wesley and A. Rich, Phys. Rev. A4 (1971) 1341.
- [13] S. Granger and G.W. Ford, Phys. Rev. Letters 26 (1971) 1351.
- [14] J. Bailey, W. Bartl, G. von Bochmann, R.C.A. Brown, F.J.M. Farley, M. Glesch, H. Jostlein, S. van der Meer, E. Picasso, and R.W. Williams, Phys. Letters 28B (1968) 287.
- [15a] T. Kinoshita and P. Cvitanovic, Phys. Rev. Letters 29 (1972) 1534.
- [15b] M.J. Levine and J. Wright, University of Illinois preprint (ILL-TH-73-5).
- [15c] R. Carroll and York-P. Yao (to be published in Phys. Letters).
- [16] B. Lautrup and E. de Rafael, Phys. Rev. 174 (1968) 1835.
- [17] B.N. Taylor, W.H. Parker and D.N. Langenberg, Rev. Mod. Phys. 41 (1969) 375.
- [18] J. Aldins, S. Brodsky, A. Dufner and T. Kinoshita, Phys. Rev. Letters 23 (1969) 441; Phys. Rev. D1 (1970) 2378.
- [19] A. Peterman, CERN-TH-1566 (Sept. 1972).
- [20] S. Adler, Phys. Rev. D5 (1972) 3021.
- [21] E. de Rafael and J.L. Rosner, CERN preprint, TH-1645 (1973) (to be published in the Ann. of Phys.).
- [22] T. Kinoshita, Cargése Lectures in theoretical physics, 1967, vol. 2, p. 209.
- [23] R. Jost and J.M. Luttinger, Helv. Phys. Acta 23 (1950) 201.
- [24] C.R. Hagen and M.A. Samuel, Phys. Rev. Letters 20 (1968) 1405.
- [25] J.L. Rosner, Phys. Rev. Letters 17 (1966) 1190; and Ann. of Phys. 44 (1967) 11.
- [26] Glen W. Erickson and Henry H.T. Liu, UCD-CNL-81 report (1968).
- [27] H. Suura and E. Wichmann, Phys. Rev. 105 (1957) 1930.
- [28] A. Petermann, Phys. Rev. 105 (1957) 1931.
- [29a] C.M. Sommerfield, Phys. Rev. 107 (1957) 328.
- [29b] A. Petermann, Helv. Phys. Acta 30(1957) 407; Nucl. Phys. 3 (1957) 689.
- [30] B.E. Lautrup and E. de Rafael, Nuovo Cimento 64A (1969) 322.
- [31] D. Billi, M. Caffo and E. Remiddi, Nuovo Cimento Letters 4 (1972) 657.
- [32] S. Barbieri, M. Caffo and E. Remiddi, Nuovo Cimento Letters (1972) 769.
- [33] T. Kinoshita, J. Math. Phys. 3 (1972) 650.
- [34] S. Weinberg, Phys. Rev. 118 (1960) 838.
- [35a] B. Lautrup, Phys. Letters 32B (1970) 627.
- [35b] S. Brodsky and T. Kinoshita, Phys. Rev. D3 (1971) 356.
- [35c] B. Lautrup, A. Petermann and E. de Rafael, Nuovo Cimento 1A (1971) 238.
- [36] H. Terazawa, Prog. Theor. Phys. 40 (1968) 830.